Journal of Power Sources 185 (2008) 1101–1106

Contents lists available at ScienceDirect

Journal of Power Sources

journal homepage: www.elsevier.com/locate/jpowsour

Distinguishing between apparent and authentic conductivity of protonic ceramic electrolytes using differential resistance analysis applied to conductivity measurements

J. Melnik, A.R. Sanger, A. Tsyganok, J.L. Luo*, K.T. Chuang

Department of Chemical and Materials Engineering, University of Alberta, Edmonton, Alberta T6G 2G6, Canada

ARTICLE INFO

Article history:
Received 17 June 2008
Received in revised form 19 July 2008
Accepted 21 July 2008
Available online 30 July 2008

Keywords:
Conductivity
Impedance spectroscopy
Solid ionic electrolyte
Proton conductors

ABSTRACT

Differential resistance analysis (DRA) is used for determination of authentic bulk conductivity of yttrium-doped barium cerate proton conductors (BCY) using electrochemical impedance spectroscopy (EIS), by eliminating all electrode and fixture resistance as well as interfacial or surface phenomena. Bulk conductivity determined using DRA in the range 500–800 °C was higher by a factor of 1.5–3 than values obtained for conductivity of the same electrolyte using EIS alone. Application of DRA with EIS provides geometrically independent conductivity values.

1. Introduction

1.1. Apparent conductivity

The power density attainable in a solid oxide fuel cell (SOFC) is a function of several factors, of which a key element is the conductivity of the ion conducting membrane. Several developments in SOFC design include minimization of the thickness of the membrane, thereby minimizing its resistance and so maximizing the current density and power density. The conductivity of the electrolyte typically initially may be determined using membranes thicker than those used in optimized SOFC architectures. Often it is assumed that the material is homogeneous in both structure and electrochemical performance throughout the entire mass of the membrane, and so the determined value for the conductivity is used to calculate predicted fuel cell performance. Then, when fuel cell performance does not match that predicted from measured conductivity data, the discrepancy may be attributed speculatively to artifacts such as interface phenomena or inconsistencies between methods of preparation, etc.

We will show now that the apparent bulk conductivity of at least one family of ionic electrolytes varies as a function of the overall thickness of the membrane, and that the effect is attributable to differences between the characteristics of the interior and surfaces of the membrane itself. The phenomenon has implications for design of SOFC.

1.2. Proton conducting perovskites as electrolytes

High temperature ionic conducting ceramic electrolytes based on doped strontium, barium, cerium and zirconium oxides of perovskite structure with predominantly proton conduction have been extensively studied since proton conductivity in $SrCeO_3$ and related perovskites at elevated temperatures in humid atmosphere was found by Iwahara et al. [1]. There are many publications concerning electrochemical properties of these solid oxide ionic semiconductors and particularly electrical conduction and proton conductivity. The intense interest in these compounds is largely driven by the variety of promising potential utility of such materials as proton conducting membranes in chemical and power industries, including: SOFC for electric power generation, hydrogen gas separation, hydrogenation/dehydrogenation of hydrocarbons, etc.

Unfortunately, until now there has been little attempt to achieve either conformity or reconciliation between the electrochemical measurements, and this is particularly so in determinations of conductivity of the above perovskites. For example, conductivity values for the most studied barium cerate perovskites varied by more than a factor of two, as exemplified by values for $BaCe_{0.9}Y_{0.1}O_{3-\delta}$ at 600 °C in humidified hydrogen atmosphere: 0.007–0.018 S cm^{-1} [2–7]. Among the most significant reasons given for causing this

* Corresponding author. Tel.: +1 780 492 2232; fax: +1 780 492 2881.
E-mail address: jingli.luo@ualberta.ca (J.L. Luo).

0378-7753/$ – see front matter © 2008 Elsevier B.V. All rights reserved.
doi:10.1016/j.jpowsour.2008.07.056

inconsistency, thus having impact on conductivity measurements, are: (i) measurement methods (two- or four-point measurements by direct or alternating current techniques); (ii) methods and conditions of preparation of electrolyte membranes; (iii) condition of the membrane's surface and applied electrodes; and (iv) the quality of contact between the membrane and electrodes. While each of these concerns is valid, but can be addressed, the factors in the third and fourth of these sets are difficult to control.

The majority of research efforts concentrated on use of the above-mentioned techniques to improve fuel cells' design and enhance efficiency of their electric performance; fewer publications addressed the problems of enhancement of quality and uniformity of conductivity measurements [8–11]. Nevertheless, uniformity and reliability of conductivity values obtained are necessary, both for characterization of electrolytes and for development of materials for commercial applications. Of particular importance are conductivity determinations of thinly layered materials.

While performing several different conductivity evaluations of proton conducting perovskite ceramics with different thickness (including thin films), we were faced with difficulties in comparing our results with the literature data. We found that there were inconsistencies not only between different sets of literature data and between our data and literature data, but also among the conductivity values we determined. Others have encountered and addressed similar problems [4,11]. One study [11] is dedicated entirely to a systematical investigation of correlation between two conductivity measurement techniques using BCY as the electrolyte: standard electrochemical impedance spectroscopy (EIS) and DRA based on resistances determined as the slopes in the ohmic region of current–voltage characteristics for specimens with different thickness.

We recognized that the inconsistencies between the determined values were a function of the thickness of membranes, and so undertook the present study.

The aim of the present work is to explain why electrolyte resistance derived from EIS does not scale directly with electrolyte thickness. Herein we describe determination of reliable values for conductivity of yttrium-doped barium cerate electrolyte (BCY) by use of DRA approach to the EIS measurements (DRA-EIS) in symmetrical cells, and we will show that the electrochemical characteristics of the surface differ significantly from those in the interior of bulk electrolyte.

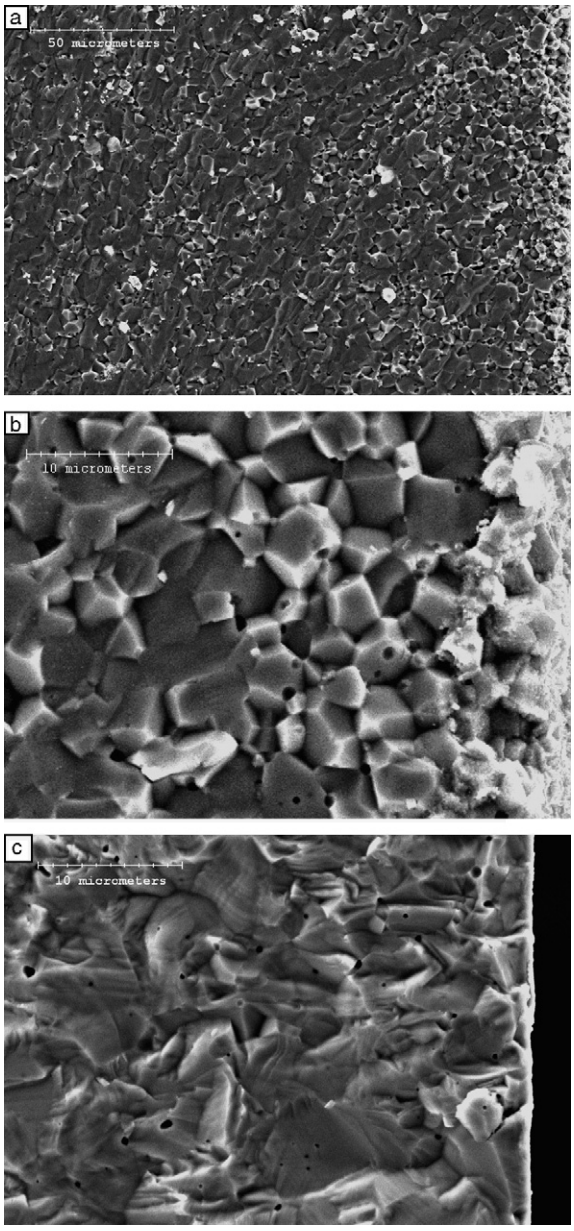

Fig. 1. SEM images of sintered BCY samples (cross-section view of fractured disks near the surface, shown on the right): (a and b) before polishing, (c) after polishing.

2. Experimental

2.1. Membranes

To assess the capability of the DRA-EIS method in a manner that enables comparison with prior studies, we chose the most commonly used method for solid state ceramic synthesis of $BaCe_{0.85}Y_{0.15}O_{3-\delta}$ (BCY) electrolyte that involved a straightforward sequence of steps: mixing precursors, calcination, specimen shaping, and sintering. Nano-powders of cerium and yttrium oxides (99.97% and 99.95% from Inframat Advanced Materials), and barium carbonate (99.98% from Aldrich) were used as precursor materials. The raw mixture of compounds prepared in designed proportion was ball-milled using zirconia balls and mill in isopropanol for 24 h, dried and calcined at 1200 °C for 10 h, reground by ball-milling, pressed at 160 MPa without any binder into disk samples 20 mm in diameter, and finally sintered at 1600 °C for 12 h in air. Both sides of each sintered disk were polished on SiC abrasive grinding paper (600 grit) to remove surface layers of any loose material or phases structurally dissimilar to inner homogeneous material that may have formed close to the surface through thermal decomposition or phase segregation. Then the thickness of the disk samples was reduced by polishing (SiC, 1200 grit) to three different values: 0.1149, 0.0716 and 0.0373 cm. The membranes were of consistent thickness within ±0.0002 cm as measured using SEM. Finally, the disks were ultrasonically cleaned in alcohol. The polished samples were screen printed with Pt paste (CL11-5100, Heraeus) on both sides with an active area of 0.3 cm^2, and heated at 950 °C for 1 h in air to provide strong bonding and good electrical contact, and to stabilize the morphology of Pt electrodes.

2.2. Cells

Symmetrical cells were assembled in two points configuration with four leads using gold meshes and wires. All measurements were conducted over the temperature range 500–800 °C in an atmosphere of hydrogen humidified by bubbling gas through

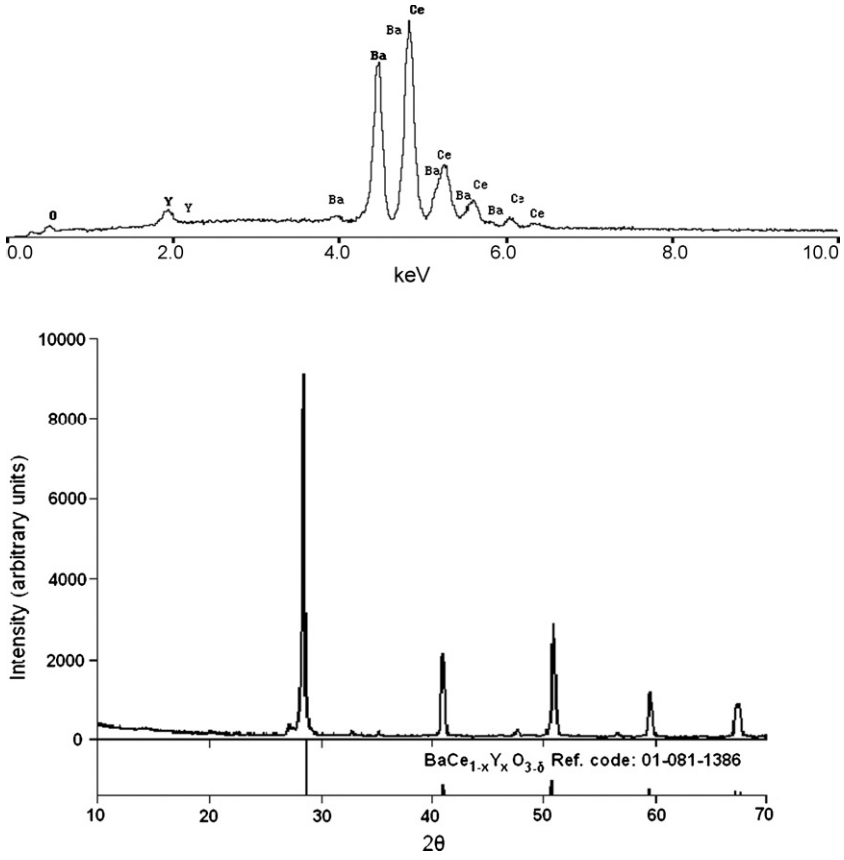

Fig. 2. EDX (above) and XRD patterns (below) of a sintered BCY sample.

water at room temperature (ca. 3% humidity). EIS measurements were performed at open circuit voltage (OCV) with 10 mV applied amplitude over the frequency range of 100 kHz to 0.1 Hz within ±0.0001 Ω using a Solartron 1255B frequency response analyzer and Solartron electrochemical interface system SI 1287. Electrical resistance of current collectors and other electric contacts and fixtures was preliminarily measured with short-circuited current collectors at appropriate temperatures in the same atmosphere. The values for the membrane then were obtained by subtracting these values for the resistance of all external conductors from the experimental values.

2.3. Analyses of materials

Microstructure and elemental composition of sintered BCY samples were determined using scanning electron microscopy (SEM) with X-ray energy dispersive analysis (EDX) using a Hitachi scanning electron microscope equipped with a PGT IMIX digital imaging system and a PGT PRISM IG detector for EDX. Phase composition of synthesized BCY was analyzed using X-ray diffraction (XRD) in Cu Kα radiation with a Rigaku Rotaflex X-ray diffractometer.

3. Results and discussion

3.1. Phase composition and microstructure characterization

Mechanically strong and dense (more than 97% of theoretical density calculated using weight and volume) BCY disk samples were prepared at relatively high sintering temperature (1600 °C) from nano-powders of starting materials. SEM images (Fig. 1) show views of materials at and near to the surface of fractured samples before (a and b) and after (c) polishing. The views show that the preparative conditions facilitated obtaining dense homogeneous microstructure, and the EDX pattern (Fig. 2) shows clearly the BCY elemental composition. The illustrated microstructures of sintered bulk materials are characteristic of full-fired ceramics without any noticeable concentration of single crystals which usually are present in BCY ceramics sintered at lower temperatures. This effect is attributed to the strong intimate contacts between crystal grains which cause primary breaking across crystals but not along the grain boundaries on the fractured sample's surface (Fig. 1b). The bulk material of the sintered ceramics appeared to comprise mainly BCY perovskite phase (XRD analysis; Fig. 2), containing traces of Y-doped ceria (ref. codes: 01-081-1386 and 01-083-0326, respectively). In contrast, in the regions located close to the sample surfaces (i.e. up to about 0.025 mm depth) there were well-formed crystal grains with sharply defined boundaries (Fig. 1a and b). Moreover, the surface exposed to ambient sintering atmosphere had obvious features of crystal degeneration caused by phase transformations and thermal decomposition. Therefore, it was crucial to reliable and reproducible performance of conductivity tests to first remove the surface layers by polishing, and this was done to prepare samples with various thicknesses. Fig. 1c shows the homogeneity of a sample in a fractured cross-section view of a polished sample with the surface layers removed.

3.2. Differential resistance analysis

Differential resistance analysis (DRA) is based on a mathematical method for mapping out a certain functional constant from the linear relationship between values of two variables. In the present case, the variables are the cell resistance (R, Ω) and thickness (d, cm)

Table 1
Area-specific resistances ($\Omega\,cm^2$) of BCY depending on thickness and temperature

Temperature (°C)	Thickness (cm)				
	0[a]	0.0373	0.0716	0.1149	1[b]
500	2.01	4.07	6.10	8.45	58.31
600	1.57	2.75	3.97	5.30	34.26
700	1.45	2.26	3.02	3.95	23.24
800	1.10	1.60	2.03	2.63	14.30

[a] Derived by extrapolation of EIS data.
[b] Calculated using DRA.

of the BCY electrolyte. Any electrode, fixture and other originally unknown resistances can be considered as a functional constant characterizing an integral resistance independent on electrolyte geometry (thickness in this case) and can be excluded from total cell resistance, thus giving reliable calculated values for the electrolyte resistance (R_e) when the electrolyte has a thickness $d^0 = 1$ cm (Eq. (1); the subscripts 1 and 2 denote values for samples of electrolyte having different thicknesses):

$$R_e = \frac{R_1 - R_2}{d_1 - d_2} \quad (1)$$

From these data, reliable values for the electrolyte conductivity (σ_e) then can be calculated using Eq. (2):

$$\sigma_e = \frac{d^0}{A_s R_e} \quad (2)$$

where $d^0 = 1$ cm; A_s is the surface area (cm^2) of an electrolyte under measurement; the product $A_s R_e$ is the area-specific resistance ASR ($\Omega\,cm^2$).

Coors and Zhong [11] applied the DRA approach to the current – voltage measurements in the hydrogen – air SOFC with BCY electrolyte to determine values for the bulk conductivity of the electrolyte. In the present study, to reduce uncontrollable uncertainties commonly encountered when using complex operating SOFC setups, we chose a simple symmetrical cell arrangement allowing direct conductivity measurements in different atmospheres using many available electrochemical measurement techniques. Herein we describe use of electrochemical impedance spectroscopy (EIS) as an accurate and highly informative method. All our tests were carried out with maximum possible care under equivalent experimental conditions. Impedance measurements were recorded after the temperature and impedance were stable, and the electrical resistance of current collectors, outer electric contacts and other fixtures were then subtracted from the overall experimental values.

In Table 1 we present area-specific resistances (ASR_0) calculated from values of first (high frequency) intercepts of impedance curves with the real impedance axis obtained from our EIS measurements for various thicknesses (d) at different temperatures that usually characterize the bulk resistance of solid electrolytes at elevated temperatures [12]. Linear extrapolation provided values corresponding to vanishingly small thicknesses of the membrane ($d = 0$ cm). Values calculated using DRA for a thickness of 1 cm also are presented in the table.

Plots of the experimental values for ASR_0 are linear within better than 0.998 mean square deviation for "resistance–thickness" relationships at different temperatures (Fig. 3). Extrapolated values for 0 cm thickness are also plotted. Since a non-trivial residue value for resistance at "zero" thickness does not make sense for bulk electrolyte characterization, these values can be attributed to electrolyte surface phenomena as well as electrode interfacial phenomena [7,13,14]. In an alternative approach, by treating the electrolyte body as a sandwich of homogeneous bulk electrolyte between two thin surface layers that are different from bulk

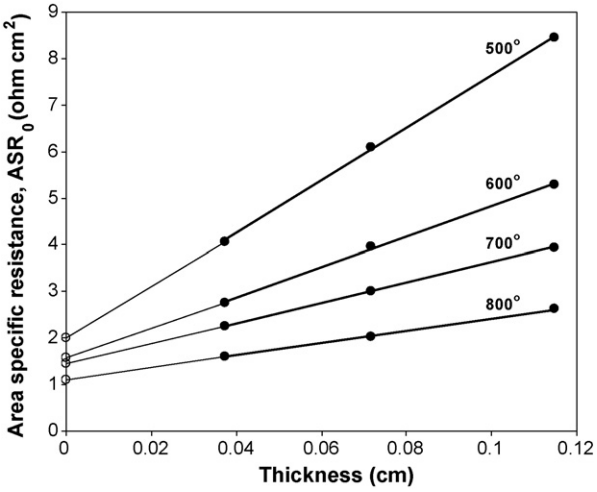

Fig. 3. Area-specific resistance of BCY samples as a function of thickness at different temperatures.

material, we can evaluate resistance (Fig. 3) and hence estimate conductivity (Fig. 4) of each of those layers no matter how thin they are. For example, if the surface layers extend to a depth of about 5 μm (the best up-to-date achievement in BCY thin film preparation [7]) the conductivity of those layers will be of the order of 10^{-4} S cm^{-1} at 500–800 °C temperature range. However, if the surface layers are, for example, 0.5 μm, then the enhanced resistance extends over a smaller distance, and so the conductivity will be an order of magnitude lower. Consequently, as there will always be the more resistive surface layers present, they will have an increasingly strong effect on the total internal resistance as the overall thickness of the membrane is reduced.

3.3. Electrochemical impedance measurements and electrolyte conductivity

EIS spectra for membranes of three different thicknesses obtained in our tests of BCY electrolyte in the symmetrical cell configuration in 500–800 °C temperature range are shown in Fig. 5. Every spectrum has two well-defined predominant arcs for all thicknesses and temperatures. At the highest temperature (800 °C) the arcs strongly overlap each other. The characteristic frequen-

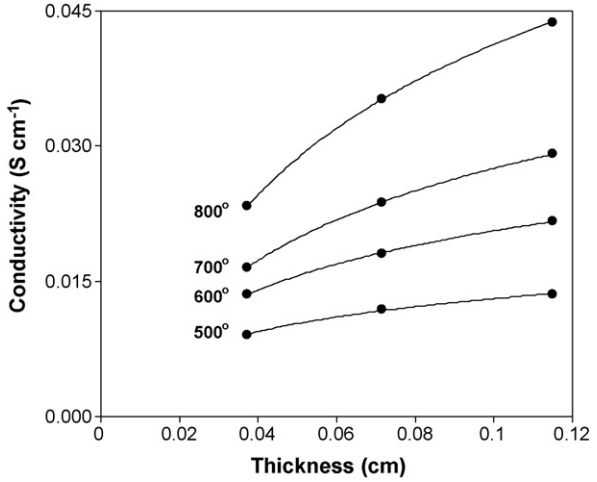

Fig. 4. Relationship between apparent conductivity and thickness of BCY membranes as a function of temperature.

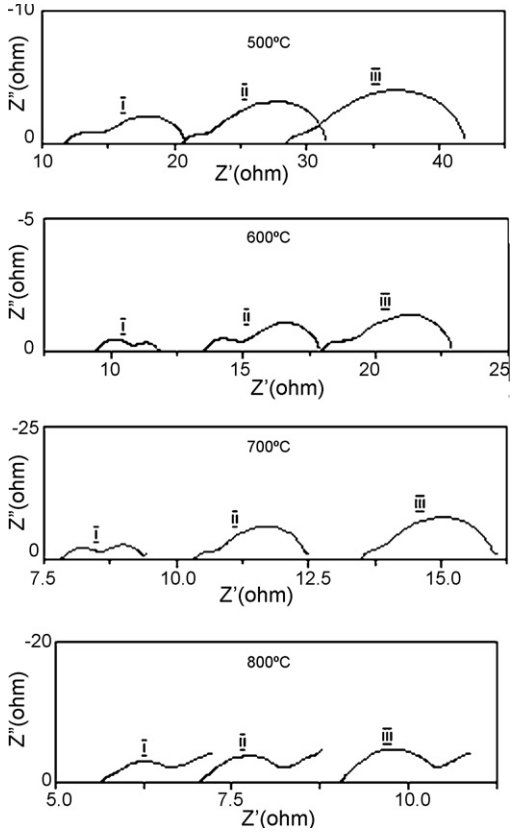

Fig. 5. Original impedance spectra of BCY electrolyte at different temperatures and thickness (I: 0.0373 cm; II: 0.0716 cm; III: 0.1149 cm).

cies for second (low-frequency) arcs are independent of thickness at constant temperature while those for first (high-frequency) arcs shift slightly to lower values with increasing thickness. Resistance of high-frequency arcs (R_1) changes a little with thickness while resistance of low-frequency arcs decreases significantly with decrease of thickness at constant temperature (Fig. 5). On the other hand, increase in temperature leads to decrease in resistances associated with both arcs. The total spectra show those features typically reported in prior impedance studies on BCY [4,8,9,12,15].

According to generally accepted approach to the impedance response of solid state electrochemical cells with polycrystalline solid ionic conductors, the low-frequency arc can be attributed to transport processes in the electrode and the electrolyte while the higher-frequency arc can imply one or both of grain boundary resistance and some medium-frequency surface kinetic processes (adsorption and dissociation) [7,12]. Resistance R_0 in the point of first intercept corresponds to the bulk resistance, as there are no other significant bulk arcs at high temperatures.

In Fig. 6 are presented Arrhenius plots for bulk conductivities calculated from our EIS experimental data and DRA, and these are each linear within better than 0.985 mean square deviation. Theoretically, conductivity does not depend on thickness, but in fact we obtained significant differences: apparent values for the conductivity increased by between 1.5 and 1.9 times (at 500 and 800 °C, respectively) when the thickness was increased by a factor of three. The apparent variability of conductivity with thickness is consistent with existence of surface characteristics and phenomena discrete from those present in the bulk material, evinced as a non-trivial value for resistance as determined from extrapolation to zero thickness.

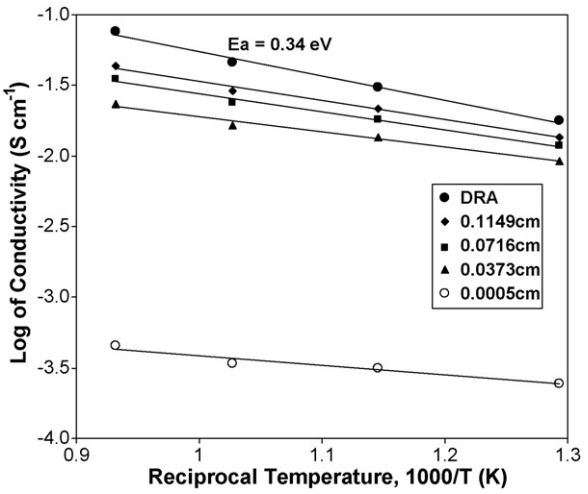

Fig. 6. Arrhenius plots for bulk conductivity of BCY membranes of various thicknesses obtained by EIS measurement, extrapolation (5 μm) and DRA calculation.

Thus, by isolating values obtained from use of different methods, consistent values can be determined for the bulk conductivity of the electrolyte, characteristic of the bulk properties of the electrolyte and independent of thickness. As described above, conductivity calculated by DRA was higher by 1.5–3 times (0.02–0.08 S cm^{-1}) when compared to overall experimental values. The DRA conductivity values were dependent only on temperature, whereas the EIS conductivity values depended on both temperature and electrolyte thickness. Thus the former, higher values are the more reliable values.

The activation energy calculated for DRA conductivity was about 0.34 eV, a value significantly lower than that reported for BCY proton conductors (about 0.5 eV) [7]. The discrepancy can be attributed to the mixed character of conduction mechanism [9] as well as the effect of very low surface activation energy. The apparent activation energy calculated for a membrane with "zero" thickness was much lower (about 0.13 eV). While the nature of such low activation energy cannot be unequivocally attributed at this time, it appears to be associated with some surface processes [14] rather than charge transfer processes in ion-conductive solid electrolytes. The SEM and XRD data do not show conclusively the physical presence of layers having different structure to that of the bulk electrolyte. However, this may be because they are very thin and indistinguishable using these techniques. Regardless of the nature of such a layer, and its cause, it is clear that this "zero layer" behaves differently from the bulk electrolyte, and that it limits conduction no matter how thin the BCY electrolyte may be prepared.

3.4. Nature of the surface resistance

There may be several contributing factors causing higher resistance at the surface of the perovskite electrolyte. The present data do not allow unequivocal allocation of cause to the effect. Nevertheless, supposing successful elimination of electrode and fixture resistances, the present data and knowledge of the structures of perovskites indicate possible causes. Here we will consider two factors: the nature of the crystal surface and the interfacial phenomena between electrolyte and electrode.

The structure of an ideal perovskite ABO_3 is cubic, space group $Pm3m$-O_h, in which the larger A^{2+} cation is 12-fold coordinated by O^{2-} ions and the smaller B^{4+} cation is sixfold coordinated [16]. The O^{2-} ions are centered along edges of the cubic structure, placed symmetrically between two B^{4+} cations. Substitution for B^{4+} cations

by other cations having a lower charge creates O^{2-} deficiencies. In such cases the O^{2-} anions are no longer exactly symmetrically situated between the different cations along an edge. These effects induce distortions of the ideal perovskite structure (orthorhombic distortion in BCY) and consequently change the physical properties, including ionic conductivity [16].

Several methods have been employed to prepare perovskites having highly ordered surface structures, including epitaxial thin film growth [e.g. 17–19]. Typically, well-ordered surfaces have terraces and steps with heights corresponding to a single cubic perovskite cell dimension (ca. 0.4 nm). In each case, the B^{4+} cations of the structures appeared to be well ordered. However, it will readily be recognized that the surface ions no longer have their full coordination number according to the structure in the bulk. Thus there is a difference in both the immediate cell at the surface and, by transmission of the electrochemical imbalance so created, those cells closely adjacent the surface.

On the other hand, an intrinsic potential barrier to migration of charge carriers between electrode and electrolyte can make a significant contribution to the surface ohmic losses observed. This limiting factor, affecting all systems, is exacerbated when the surface layer of one phase has reduced capacity for conduction.

In either case, the residual surface resistance, either from uncompensated surface crystal structure of the electrolyte or from the potential barrier between the electrolyte and the electrode material, will result in change in conductivity of the surface layer.

The determinations made herein and by others show that the conductivities of surface layers and bulk electrolytes can differ considerably. In this case the surface had lower conductivity than the bulk. It can reasonable be expected that in other cases the surface may be more conductive than bulk electrolyte. Consequently, we advocate that all investigations including determinations of ionic conductivity be performed on a minimum of two samples of different thickness. When the intercept of the plot of apparent conductivity versus thickness does not intercept the axis close to the origin it will indicate that the surface and bulk differ in conductivity. An intercept above the origin will imply that the surface has low conductivity, and so the material should be carefully reconsidered before use in thin membranes. In contrast, an intercept below the origin will indicate that the surface has higher conductivity than the bulk, and so that electrolyte may be a good candidate for preparation of very thin membranes.

4. Conclusions

Comparison and correlation of data obtained using differential resistance analysis and electrochemical impedance spectroscopy showed that the former can be employed to distinguish between the authentic, geometrically independent conductivity of the majority internal bulk of a solid ionic electrolyte and the apparent values from determination of the resistance of the overall structure, and so obtain bulk conductivity characteristics independent of membrane thickness.

Values for conductivity of barium cerate based proton conductors calculated using differential resistance analysis of electrochemical impedance spectroscopy data differ from those derived from EIS only. The EIS conductivity increased by a factor of 1.5–2 when the thickness increased threefold, in apparent contradiction to authentic electrolyte conductivity being thickness-independent. The differences in values are attributable to the certain residual resistance that limits the overall conduction of electrolyte membranes and films no matter how thin they are.

Values for conductivity of the internal bulk of the electrolyte calculated using differential resistance analysis are between 1.5 and 3 times higher than apparent values obtained for the whole membrane over the range 500–800 °C.

Conductivity determinations must be performed on at least two membranes having different thickness to show whether or not the conductivities of the surface and bulk differ.

Acknowledgments

The authors would like to thank the Natural Science and Engineering Council of Canada, Strategic Program Grant, for financial support and V. Vorontsov and Dr. E. Zholkovskiy for helpful discussions.

References

[1] H. Iwahara, T. Esaka, H. Uchida, N. Maeda, Solid State Ionics 3–4 (1981) 359–363.
[2] N. Bonanos, B. Ellis, K.S. Knight, M.N. Mahood, Solid State Ionics 35 (1989) 179–188.
[3] K. Katahira, Y. Kohchi, T. Shimura, H. Iwahara, Solid State Ionics 138 (2000) 91–98.
[4] W.G. Coors, D.W. Readey, J. Am. Ceram. Soc. 85 (2002) 2637–2640.
[5] G. Ma, T. Shimura, H. Iwahara, Solid State Ionics 110 (1998) 103–110.
[6] K.D. Kreuer, Annu. Rev. Mater. Res. (2003) 333–359.
[7] F. Sammels, M.V. Mundschau, Nonporous Inorganic Membranes, Wiley-VCH, Verlag GmbH & KGaA, Weinheim, 2006, pp. 49–73.
[8] W.G. Coors, R. Swartzlander, Proceedings of the 26th Risø International Symposium on Materials Science, Solid State Electrochemistry, Roskilde, Denmark, September 4–8, 2005, pp. 185–196.
[9] W. Suksamai, I.S. Metcalfe, Solid State Ionics 178 (2007) 627–634.
[10] J. Guan, S.E. Dorris, U. Balachardran, M. Liub, Solid State Ionics 100 (1997) 45–52.
[11] W.G. Coors, D. Zhong, Solid State Ionics 162–163 (2003) 283–290.
[12] S.P. Jiang, J.G. Love, S.P.S. Badwal, Key Eng. Mater. 125–126 (1997) 81–132.
[13] H.J.M. Bouwmeester, H. Kruidhof, A.J. Burggraaf, Solid State Ionics 72 (1994) 185–194.
[14] A. Tomito, T. Hibino, M. Suzuki, M. Sano, J. Mater. Sci. 39 (2004) 2493–2497.
[15] H.G. Bohn, T. Schober, J. Am. Ceram. Soc. 83 (2000) 768–772.
[16] M.A. Pena, J.L.G. Fierro, Chem. Rev. 101 (2001) 1981–2017.
[17] H. Tanaka, H. Tabata, Thin Solid Films 342 (1999) 4–7.
[18] J.A. Agostinelli, S. Chen, United States Patent 5,128,316 (1992).
[19] J.A. Agostinelli, S. Chen, United States Patent 5,241,191 (1993).